2D Materials

PAPER

Centimeter-scale, single-crystalline, AB-stacked bilayer graphene on insulating substrates

RECEIVED
18 June 2019

REVISED
21 August 2019

ACCEPTED FOR PUBLICATION
27 August 2019

PUBLISHED
6 September 2019

Hui Guo[1,4], Xueyan Wang[1,4], Hongliang Lu[1,2,4], Lihong Bao[1], Hao Peng[1], Kai Qian[1], Jiajun Ma[1], Geng Li[1], Li Huang[1], Xiao Lin[1,2], Yu-Yang Zhang[1,2], Shixuan Du[1,2], Sokrates T Pantelides[1,3] and Hong-Jun Gao[1,2]

[1] Institute of Physics and University of Chinese Academy of Sciences, Chinese Academy of Sciences, Beijing 100190, People's Republic of China
[2] CAS Center for Excellence in Topological Quantum Computation, University of Chinese Academy of Sciences, Beijing 100190, People's Republic of China
[3] Department of Physics and Astronomy and Department of Electrical Engineering and Computer Science, Vanderbilt University, Nashville, TN 37235, United States of America
[4] The authors (HG, XYW, and HLL) contributed equally to this work.

E-mail: lhbao@iphy.ac.cn **and** zhangyuyang@ucas.ac.cn

Keywords: bilayer graphene, centimeter-scale, insulating substrate, intercalation, Ru crystal

Supplementary material for this article is available online

Abstract

Bilayer graphene (BLG) attracts great interest in both scientific research and potential applications. To achieve integrated applications of functional devices, synthesis of large-scale, single-crystalline BLG with a controlled stacking structure on insulating substrates is highly desired. However, so far, only polycrystalline BLG has been fabricated on insulating substrates, with single-crystalline domains limited to about half a millimeter. Here, we demonstrate successful fabrication of centimeter-scale, single-crystalline AB-stacked BLG on insulating substrates. First, we epitaxially grow single-crystalline BLG on Ru(0 0 0 1) and then transfer it to insulating substrates by an oxygen-intercalation-assisted electrochemical approach. The oxygen atoms intercalated between the BLG and Ru effectively decouple the BLG from Ru, enabling its successful transfer to a SiO_2 substrate, which makes it readily available to Si-based technologies. Low-energy electron diffraction, scanning tunneling microscopy, and optical characterization demonstrate that the BLG on SiO_2 is centimeter-scale, single-crystalline, and AB-stacking. The carrier mobility is measured at about 2000 $cm^2 V^{-1} s^{-1}$. This work provides a promising platform for future applications of large-scale, single-crystalline, high-quality BLG.

1. Introduction

Bilayer graphene (BLG), consisting of two graphene monolayers, has attracted significant attention due to its extraordinary physical properties as well as potential applications in devices [1]. With different stacking configurations, plenty of exotic phenomena, such as van Hove singularities [2, 3], twist-angle-dependent electronic states [4, 5], Mott insulating behavior [6], and unconventional superconductivity [7], have been discovered in BLG. Of particular interest, Bernal (AB)-stacked BLG has a non-zero band gap [8–13], which makes BLG a promising candidate for applications in electronic and optoelectronic devices [14–16]. To achieve the integration of BLG-based functional devices, large-scale, high-quality BLG with a controlled stacking configuration on insulating substrates, especially on SiO_2 for compatibility with Si technology, is highly desired.

It has been reported that BLG can be directly grown on insulating substrates [17, 18]. The resulting BLG is polycrystalline with typical single-crystalline domains of order 100 μm with a random distribution of twist angles between 0 and 30° [17, 18]. An alternative way is to grow BLG on metal substrates and subsequently transfer it to insulating substrates. Copper is a widely used substrate to grow BLG [19–25]. A well-known challenge for the growth of BLG on Cu is to overcome the self-limiting effect, i.e. upon formation of the first graphene layer, the catalytic breakdown of hydrocarbons is not as effective for the formation of the second [26]. So far, the BLG transferred to insulating substrates can be wafer-scale with a polycrystalline structure [19, 25, 27]. The reported single-crystalline BLG

domains in AB-stacking have a size that varies from few micrometers to about half-millimeter [20–25, 28, 29]. Compared to Cu, bulk Ru has a relatively large carbon solubility [30, 31], enabling it to overcome the self-limiting effect through the segregation of carbon atoms from the bulk to the surface. The Ru crystal is demonstrated to be an ideal substrate to grow large-area, single-crystalline graphene [32–34] in a controllable, layer-by-layer mode [35, 36]. However, due to strong graphene-Ru coupling, the successful transfer of large-scale BLG grown on Ru to insulating substrates is still an open challenge.

In this paper, we report successful fabrication of centimeter-scale, single-crystalline, AB-stacked BLG on a SiO_2 substrate by first growing the BLG on a clean Ru (0 0 0 1) substrate and then transferring it to the SiO_2 substrate by an oxygen-intercalation-assisted electrochemical transfer method. Low-energy electron diffraction (LEED) patterns show sharp diffraction spots of graphene while scanning tunneling microscopy (STM) images reveal a defect-free atomic structure, proving the high quality of the as-prepared BLG. Then, oxygen intercalation at the interface between BLG and Ru substrate is performed. The intercalated oxygen atoms effectively decouple the BLG from Ru, which renders the BLG effectively freestanding, facilitating the transfer process. The entire decoupled BLG film on the Ru substrate is transferred to a SiO_2 substrate with minimal damage by means of the standard electrochemical hydrogen-bubbling method. LEED and STM measurements on the transferred BLG on SiO_2 reveal its high-quality and single-crystalline properties. Raman characterization demonstrates that the BLG is centimeter-scale and AB-stacking. The measured carrier mobility of the BLG on SiO_2 substrates is approximately 2000 $cm^2\ V^{-1}\ s^{-1}$, showing a high electronic quality. The original Ru substrate can be cleaned and used again without loss of BLG quality, whereby the process is scalable and promising for applications.

2. Methods

2.1. Sample fabrication

BLG growth and oxygen intercalation were carried out in a home-built ultra-high vacuum (UHV) MBE system with a base pressure of about 2×10^{-9} mbar. First, a Ru(0 0 0 1) surface was cleaned by repeated cycles of sputtering and annealing. The size of the Ru crystal used in this work is 0.8 cm × 0.8 cm. Large-scale, high-quality BLG was fabricated by exposing ethylene up to a pressure of 3×10^{-6} mbar at 1420 K for 150 s, followed with cooling down to room temperature at a slow rate of about 60 K min^{-1}. The annealing temperature of the Ru(0 0 0 1) substrate is the most important parameter for the growth of BLG. Unlike the growth temperature of ~1100 K for monolayer graphene that was used in [33], here the elevated growth temperature of 1420 K increases carbon solubility in bulk Ru, favouring the growth of uniform BLG. At these conditions, the grown BLG layer covers the entire Ru surface. Oxygen intercalation below the entire BLG layer was achieved by in-situ exposing BLG/Ru to oxygen at a pressure of 1×10^{-5} mbar at about 600 K. The oxygen-intercalated BLG was spin-coated with PMMA (950 kDa molecular weight, 5 wt.% in ethyl lactate) at 2000 r.p.m. for 1 min followed by baking at 180 °C for 30 min. The PMMA-coated sample was then dipped into a 1M NaOH aqueous solution and used as a cathode with an applied electrolytic voltage around 1.9 V. The hydrogen bubbles were gradually generated and delaminated PMMA/BLG film from the Ru substrate. When the PMMA/BLG film was fully separated from Ru, it was picked up and transferred to a target substrate and all the PMMA was removed with acetone.

2.2. Characterization

STM images for Gr/Ru and Gr/O/Ru were obtained at about 4 K. STM images of BLG on SiO_2 substrate were obtained in a home-built four-probe STM system at room temperature. LEED was employed with a four-grid detector (Omicron Spectra LEED) in the UHV chamber. Graphene is grounded when LEED measurement is performed. Raman spectra and maps were obtained by a commercial confocal Raman microscope (WiTec), using an excitation wavelength of 532 nm and power of 1 mW. Back-gate field-effect transistors were fabricated by a standard electron-beam lithography technique followed by e-beam evaporation of Cr/Au (5/60 nm) as contact electrodes. All electrical measurements were carried out in a vacuum chamber with the pressure lower than 10^{-5} mbar, using a Keithley 4200-SCS system.

3. Results and discussion

Figures 1(a)–(c) show a schematic to illustrate the fabrication process of centimeter-scale BLG on insulating substrates. First, single-crystalline BLG is grown on a clean Ru(0 0 0 1) surface by molecular beam epitaxy (MBE) (figure 1(a)). At optimized growth conditions (see methods), a BLG layer can extend over the entire Ru surface (0.8 cm × 0.8 cm in this case). *The size of the fabricated BLG is, therefore, determined by the size of the Ru substrate.* To further realize a large-scale transfer of the grown BLG from Ru to insulating substrates, first weakening the interaction between the BLG and Ru is crucial. Intercalation is proven to be an effective way to decouple graphene from metal substrates [37]. A subsequent intercalation of oxygen at the interface of BLG/Ru decouples the epitaxial BLG from Ru substrate (figure 1(b)). Then, the decoupled BLG is transferred from Ru to an insulating substrate by a standard electrochemical hydrogen-bubbling method [38] (figure 1(c)). Figure 1(d) is a digital photograph of the transferred BLG on a SiO_2

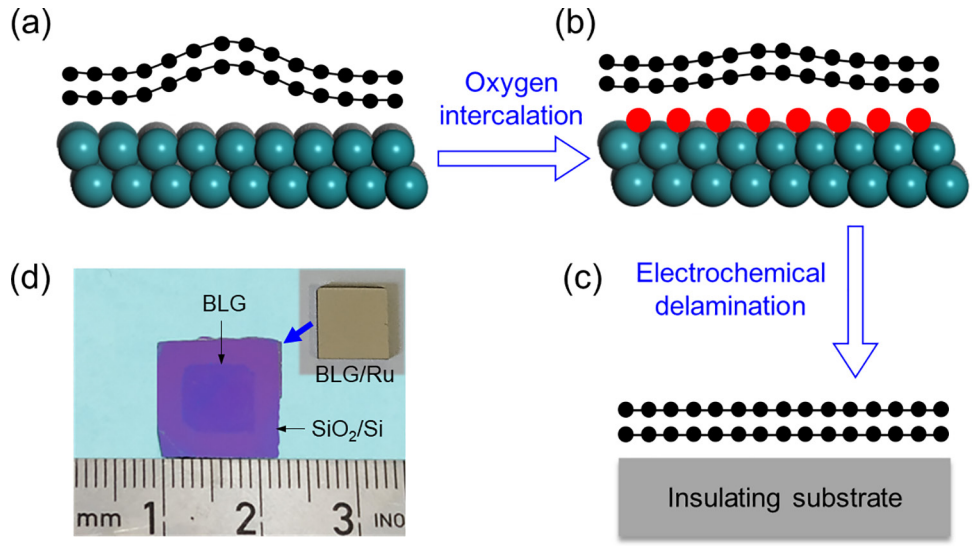

Figure 1. Schematic diagram of the fabrication process of the large-scale BLG on insulating substrates. (a) Large-scale, single-crystalline epitaxial BLG on Ru(0 0 0 1). (b) Oxygen intercalation at the BLG-Ru interface. (c) Transfer of BLG from Ru to SiO_2/Si substrate by electrochemical delamination. (d) A digital photograph of the transferred BLG on SiO_2/Si substrate. Inset: a photograph of the BLG on a 0.8 cm × 0.8 cm Ru(0 0 0 1) (before transfer).

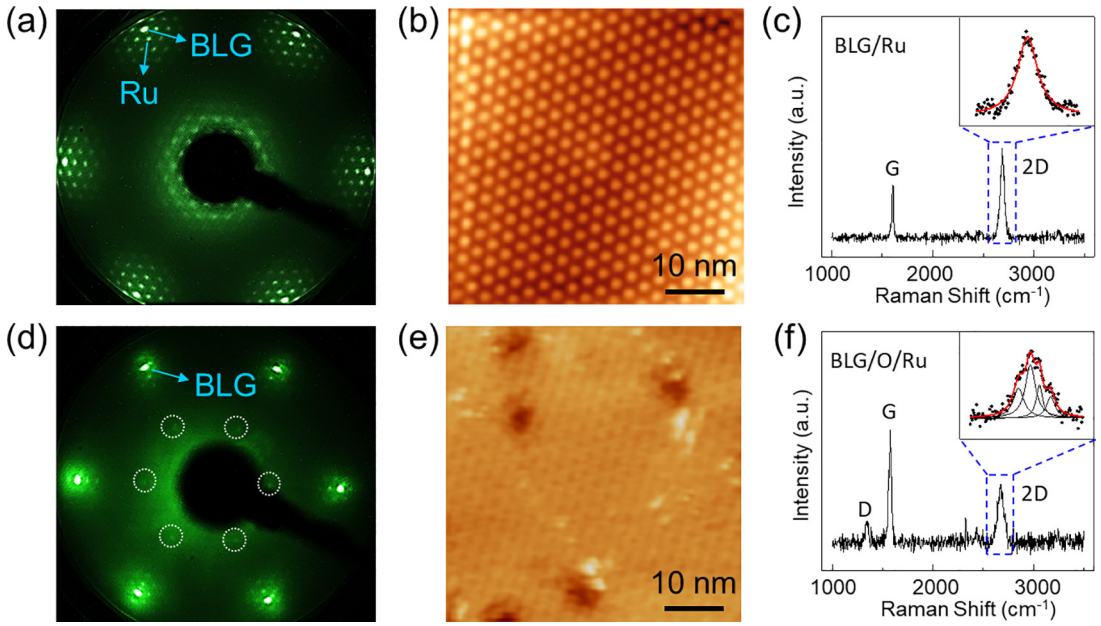

Figure 2. BLG before and after oxygen intercalation. (a) A LEED pattern of epitaxial BLG on Ru(0 0 0 1). (b) A STM ($V_s = -1$ V, $I_t = 100$ pA) image of BLG. The spots correspond to the moiré pattern with a 3 nm periodicity. (c) Raman spectrum of BLG/Ru; inset is the 2D band, well fitted by a single Lorentzian peak. (d) A LEED pattern of BLG after oxygen intercalation, showing a 2 × 2 superstructure (indicated by white circles) with respect to Ru(0 0 0 1). (e) The corresponding STM image ($V_s = -0.5$ V, $I_t = 500$ pA). (f) Raman spectrum of BLG/O/Ru; inset is the 2D band, well fitted by four narrow Lorentzian components.

substrate, showing the BLG has a size of about 0.8 cm × 0.8 cm. Compared to the size of the growth substrate (Ru), as shown in the inset of figure 1(d), it is clear that the whole fabricated BLG is separated from Ru by the intercalation-assisted transfer method.

LEED, STM, and Raman spectroscopy are employed to characterize the as-prepared BLG/Ru and oxygen-intercalated BLG/Ru samples (BLG/O/Ru). Figure 2(a) is the LEED pattern of BLG/Ru, showing sharp diffraction spots from BLG and the surrounding satellite spots from the moiré pattern. The two graphene layers in BLG generate a single set of diffraction spots that aligns to the Ru(0 0 0 1) lattice vector without a rotation angle. The individual LEED pattern obtained at different positions across the entire sample surface remains unchanged (figure S1), indicating a large-scale and single-crystalline BLG. A large-scale STM image in figure S2 shows that there are no monolayer or trilayer graphene islands. From high-resolution STM image in figure 2(b), we clearly see a defect-free graphene moiré pattern with a periodicity of about 3 nm.

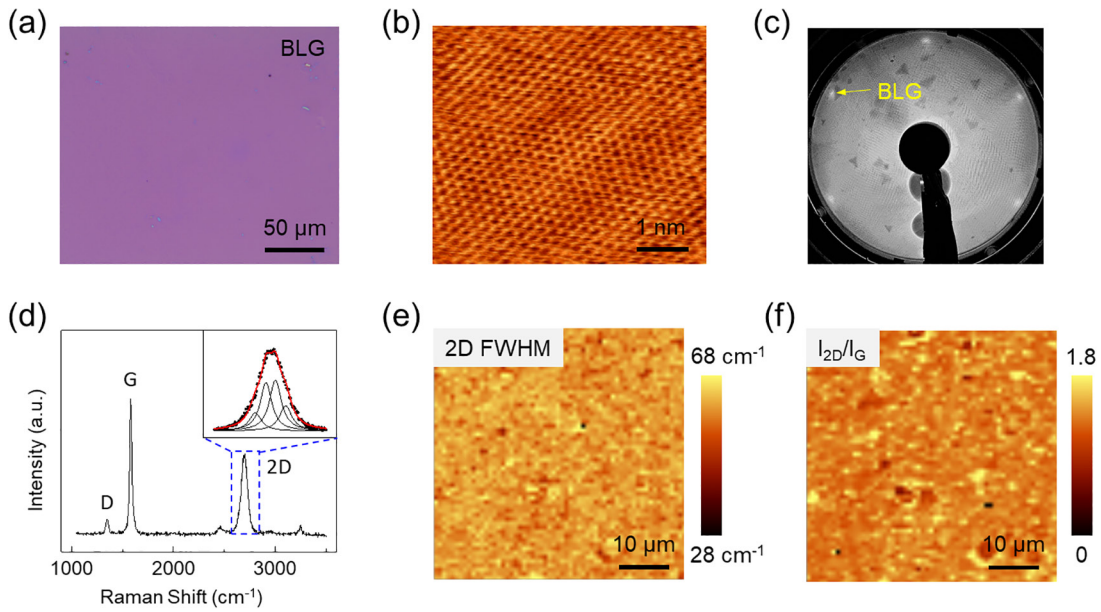

Figure 3. Properties of the transferred BLG on a SiO_2/Si substrate. (a) An optical image of the transferred BLG. (b) An atomic-resolved STM image ($V_s = -0.3$ V, $I_t = 3.5$ nA). (c) A LEED pattern. (d) Raman spectrum. Inset shows the fit of the 2D band. (e) and (f) Raman maps (50 μm $\times$ 50 μm) for the FWHM of the 2D band and the integrated intensity ratio of 2D to G bands (I_{2D}/I_G), respectively.

To further check the quality of the as-fabricated BLG on Ru, we performed Raman spectra measurements. Raman spectra of single-layer graphene (SLG) on Ru are known to show no detectable signal due to the strong graphene-Ru coupling, while BLG on Ru shows Raman features of SLG [39]. The Raman spectrum of the as-grown graphene (BLG/Ru sample) is shown in figure 2(c), exhibiting strong G and 2D bands. The 2D band is well fitted by a single narrow Lorentzian peak with full-width at half-maximum (FWHM) less than 40 cm^{-1}. Moreover, a 9 μm $\times$ 9 μm Raman map shows that the integrated intensity ratio of the 2D to the G peak (I_{2D}/I_G) is around 2 (see figure S3). These results suggest the spectra reveal BLG/Ru because the bottom graphene layer, as a buffer layer, effectively eliminates the interaction of the top layer with the Ru substrate. The 2D band shows the typical Raman vibrational feature of SLG instead of BLG [36]. The absence of a D peak around 1350 cm^{-1} indicates the high quality of the as-grown BLG. LEED, STM and Raman spectroscopy strongly indicate that the as-fabricated BLG is homogeneous at their respective length scales.

After exposing the BLG/Ru sample to oxygen at about 600 K, the LEED pattern changes significantly, as shown in figure 2(d). The set of diffraction spots from BLG retains high intensity, whereas the spots from the moiré pattern become weak. In addition, a group of new spots with 2 $\times$ 2 periodicity marked by the white circles emerge. Such superstructure is identical to that of oxygen chemisorbed on a Ru(0 0 0 1) surface [40]. Combining with the x-ray photoelectron spectroscopy (XPS) of the O 1*s* core-level (530.1 eV), as shown in figure S4(a), we conclude that oxygen atoms are intercalated at the BLG-Ru interface. We also performed STM measurements to confirm the oxygen intercalation. Figure S4(b) shows a large-scale STM image, where we clearly see that the Moiré pattern in partial areas almost disappears, suggesting the success of the oxygen intercalation. As more oxygen atoms are intercalated, the whole BLG becomes flat, as shown in the STM image in figure 2(e).

Raman spectra can sensitively reflect the change of the electronic states of graphene. Figure 2(f) shows the Raman spectrum of an oxygen-intercalated BLG/O/Ru sample. The integrated intensity ratio of 2D to G, I_{2D}/I_G, is reduced to around 1. The 2D band, with a FWHM about 60 cm^{-1}, is well fitted by four narrow Lorentzian components (inset of figure 2(f)). These results indicate that the BLG recovers as nearly free-standing after oxygen intercalation [41, 42]. The emergence of a weak D peak ($I_D/I_G < 0.3$) suggests a few defects in BLG, which may be caused by the inevitable oxygen etching during the intercalation process [43]. The results from LEED, STM, and Raman give strong evidence that the oxygen is intercalated beneath the entire BLG film, effectively decoupling the interaction between the BLG and Ru substrate.

The decoupling of the graphene-Ru interaction facilitates the BLG transfer process. By performing a standard electrochemical bubbling method [38], the transfer of a large-scale BLG from Ru to a SiO_2 substrate has been achieved. An optical image of the transferred BLG is shown in figure 3(a), demonstrating that the BLG is homogeneous. In contrast, without the oxygen intercalation process, the transferred BLG is typically small flakes (see discussion in figure S5). Figure 3(b) is an atomic-resolution STM image, obtained by a home-built four-probe STM system [44], demonstrating that the hexagonal lattice of the top gra-

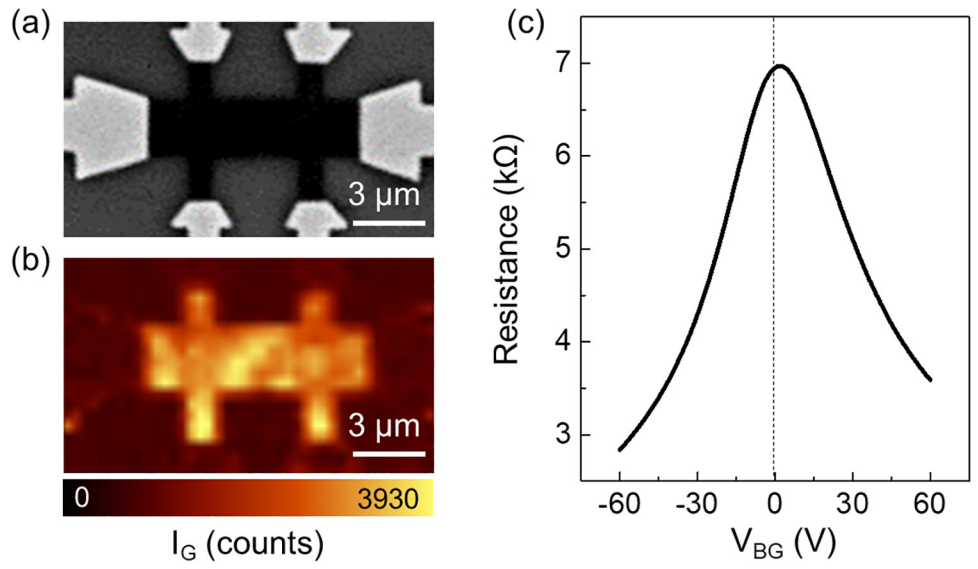

Figure 4. Transport properties of the transferred BLG on SiO_2. (a) SEM image of a back-gate field-effect transistor. (b) The corresponding G peak intensity Raman mapping of the device channel. (c) Device resistance versus back-gate voltage (V_{BG}) at room temperature. The extracted carrier mobility is about 2000 $cm^2 V^{-1} s^{-1}$.

phene layer remains intact after transfer (the bottom layer is not discernible in the images). The STM image, however, is complemented by a LEED pattern of the transferred BLG, shown in figure 3(c). Only one set of diffraction spots contributed from graphene are observed, indicating that the BLG is single-crystalline.

Raman spectroscopy is employed to evaluate the stacking order of the transferred graphene [41, 42]. In the typical Raman spectrum (figure 3(d)), the peaks of G and 2D bands are centered at 1582 cm^{-1} and 2693 cm^{-1}, respectively, which are consistent with those of exfoliated BLG on SiO_2 [42]. The integrated intensity ratio of D to G bands, I_D/I_G, is mainly around 0.21 (see figure S6), reflecting the small defect density in the transferred BLG. Raman maps of FWHM of 2D and I_{2D}/I_G are shown in figures 3(e) and (f), respectively. The corresponding distribution histograms are presented in figure S7. The 2D band with a FWHM of around 60 cm^{-1} is well fitted by four narrow Lorentzian peaks. The I_{2D}/I_G values calculated by using peak area are mainly around 1.1 (figure 3(f)) and the values calculated by using peak height are around 0.7 (figure S8). Both results confirm that the transferred BLG from Ru has AB-stacking [28, 41, 42, 45]. Optical characterizations together with LEED, STM, and Raman measurements demonstrate that we have centimeter-scale, AB-stacked, single-crystalline BLG on an insulating SiO_2 substrate.

To demonstrate an application of the centimeter-scale, high-quality, single-crystalline BLG, we fabricated back-gate field-effect transistors and performed transport measurements. Figure 4(a) displays a scanning-electron-microscopy (SEM) image of one such device. The corresponding Raman map (figure 4(b)) of the G-peak intensity clearly shows the device channel. The resistance as a function of back-gate voltage is shown in figure 4(c). We observe the Dirac point at a back-gate voltage of about 2 V in several similar devices. The extracted carrier mobility is around 2000 $cm^2 V^{-1} s^{-1}$ at room temperature, showing a high electron quality of the BLG. We compared the results in this work to some previous reports (see table S1) [18–23, 25, 27–29, 46, 47]. The carrier mobility is comparable to most reported values while the size of single-crystalline AB-stacking BLG domain is much larger than in CVD-grown BLG. Considering sample size, crystallinity, and carrier mobility, we believe the present fabricated BLG provides a better platform for scalable applications.

It is also worth noting that, after the BLG transfer, the Ru(0001) substrate is reusable. Atomic force microscopy (AFM) measurements are performed on the original Ru substrate and the same Ru substrate after the BLG transfer process (see figure S9). It is found that the atomic terraces are maintained after the transfer process. After cycles of sputtering and annealing treatments in a UHV chamber, we successfully grew high-quality BLG on the reused Ru substrate (see figure S9).

4. Conclusions

We have successfully fabricated centimeter-scale, AB-stacked, single-crystalline BLG, first on Ru(0001) and then transferred to SiO_2. The BLG epitaxially grown on a Ru(0001) substrate is characterized by LEED and STM. To achieve large-scale transfer of the as-grown BLG from Ru to other substrates, we used an intercalation-assisted electrochemical transfer method. Oxygen atoms are intercalated at the BLG-Ru interface, chemisorbing on Ru(0001) surface and forming a 2×2 superstructure. The intercalated oxygen effectively weakens the interaction between BLG and Ru, facilitating the transfer process. The entire

decoupled BLG is then transferred to a SiO_2 substrate with minimal damage by an electrochemical approach. LEED, STM, and Raman spectroscopy measurements reveal that the transferred centimeter-scale BLG is single-crystalline and AB-stacking. The carrier mobility obtained from transport measurements is around 2000 cm^2 V^{-1} s^{-1}, showing high electronic quality. The Ru substrate can be cleaned and reused without loss to the BLG quality. The present work paves a way to future applications based on large-scale and high-quality single-crystalline BLG and also extends the route of transfer of graphene from substrates with which it interacts strongly.

Acknowledgments

This work was supported by the grants from National Key Research & Development Projects of China (Nos. 2016YFA0202300 and 2018YFA0305800), National Natural Science Foundation of China (Nos. 61888102 and 51872284), the Chinese Academy of Sciences (CAS) Pioneer Hundred Talents Program, the Strategic Priority Research Program of Chinese Academy of Sciences (Nos. XDB30000000, XDB28000000), Youth Innovation Promotion Association of CAS (No. 20150005), Beijing Nova Program, China (No. Z181100006218023), and the University of Chinese Academy of Sciences. Work at Vanderbilt (STP) was supported by the McMinn Endowment. A portion of the research was performed in CAS Key Laboratory of Vacuum Physics.

ORCID iDs

Lihong Bao https://orcid.org/0000-0002-2942-892X
Geng Li https://orcid.org/0000-0002-3347-7222
Hong-Jun Gao https://orcid.org/0000-0002-2088-0522

References

[1] Yan H G 2015 *Nanophotonics* **4** 115–27
[2] Liao L, Wang H, Peng H, Yin J B, Koh A L, Chen Y L, Xie Q, Peng H L and Liu Z F 2015 *Nano Lett.* **15** 5585–9
[3] Tan Z J *et al* 2016 *ACS Nano* **10** 6725–30
[4] Koren E, Leven I, Lörtscher E, Knoll A, Hod O and Duerig U 2016 *Nat. Nanotechnol.* **11** 752–7
[5] Mele E J 2010 *Phys. Rev.* B **81** 161405
[6] Cao Y *et al* 2018 *Nature* **556** 80–4
[7] Cao Y, Fatemi V, Fang S, Watanabe K, Taniguchi T, Kaxiras E and Jarillo-Herrero P 2018 *Nature* **556** 43–50
[8] Ohta T, Bostwick A, Seyller T, Horn K and Rotenberg E 2006 *Science* **313** 951–4
[9] Zhang Y B, Tang T T, Girit C, Hao Z, Martin M C, Zettl A, Crommie M F, Shen Y R and Wang F 2009 *Nature* **459** 820–3
[10] Castro E V, Novoselov K S, Morozov S V, Peres N M R, Lopes dos Santos J M B, Nilsson J, Guinea F, Geim A K and Castro Neto A H 2007 *Phys. Rev. Lett.* **99** 216802
[11] Oostinga J B, Heersche H B, Liu X L, Morpurgo A F and Vandersypen L M K 2008 *Nat. Mater.* **7** 151–7
[12] Park J *et al* 2012 *Adv. Mater.* **24** 407–11
[13] Min H, Sahu B, Banerjee S K and MacDonald A H 2007 *Phys. Rev.* B **75** 155115
[14] Lee S Y, Duong D L, Vu Q A, Jin Y, Kim P and Lee Y H 2015 *ACS Nano* **9** 9034–42
[15] Xia F N, Farmer D B, Lin Y M and Avouris P 2010 *Nano Lett.* **10** 715–8
[16] Yan J, Kim M H, Elle J A, Sushkov A B, Jenkins G S, Milchberg H M, Fuhrer M S and Drew H D 2012 *Nat. Nanotechnol.* **7** 472–8
[17] Yan Z, Peng Z W, Sun Z Z, Yao J, Zhu Y, Liu Z, Ajayan P M and Tour J M 2011 *ACS Nano* **5** 8187–92
[18] Peng Z W, Yan Z, Sun Z Z and Tour J M 2011 *ACS Nano* **5** 8241–7
[19] Lee S, Lee K and Zhong Z H 2010 *Nano Lett.* **10** 4702–7
[20] Zhou H L, Yu W J, Liu L X, Cheng R, Chen Y, Huang X Q, Liu Y, Wang Y, Huang Y and Duan X F 2013 *Nat. Commun.* **4** 2096
[21] Hao Y F *et al* 2016 *Nat. Nanotechnol.* **11** 426–31
[22] Liu L X, Zhou H L, Cheng R, Yu W J, Liu Y, Chen Y, Shaw J, Zhong X, Huang Y and Duan X F 2012 *ACS Nano* **6** 8241–9
[23] Yan K, Peng H L, Zhou Y, Li H and Liu Z F 2011 *Nano Lett.* **11** 1106–10
[24] Zhao P, Kim S, Chen X, Einarsson E, Wang M, Song Y N, Wang H T, Chiashi S, Xiang R and Maruyama S 2014 *ACS Nano* **8** 11631–8
[25] Wu J *et al* 2017 *Adv. Funct. Mater.* **27** 1605927
[26] Li X S *et al* 2009 *Science* **324** 1312–4
[27] Liu W, Kraemer S, Sarkar D, Li H, Ajayan P M and Banerjee K 2014 *Chem. Mater.* **26** 907–15
[28] Gao Z L *et al* 2018 *ACS Nano* **12** 2275–82
[29] Yang C, Wu T R, Wang H M, Zhang G H, Sun J L, Lu G Y, Niu T C, Li A, Xie X M and Jiang M H 2016 *Small* **12** 2009–13
[30] Arnoult W J and McLellan R B 1972 *Scr. Metall.* **6** 1013–8
[31] McLellan R B 1969 *Scr. Metall.* **3** 389–91
[32] Pan Y, Shi D X and Gao H J 2007 *Chin. Phys.* **16** 3151–3
[33] Pan Y, Zhang H G, Shi D X, Sun J T, Du S X, Liu F and Gao H J 2009 *Adv. Mater.* **21** 2777–80
[34] Que Y D, Xiao W D, Fei X M, Chen H, Huang L, Du S X and Gao H J 2014 *Appl. Phys. Lett.* **104** 093110
[35] Cui Y, Fu Q and Bao X H 2010 *Phys. Chem. Chem. Phys.* **12** 5053–7
[36] Sutter P W, Flege J I and Sutter E A 2008 *Nat. Mater.* **7** 406–11
[37] Li G, Zhang Y Y, Guo H, Huang L, Lu H L, Lin X, Wang Y L, Du S X and Gao H J 2018 *Chem. Soc. Rev.* **47** 6073–100
[38] Gao L B *et al* 2012 *Nat. Commun.* **3** 699
[39] Xu W Y, Huang L, Que Y D, Li E, Zhang H G, Lin X, Wang Y L, Du S X and Gao H J 2014 *Chin. Phys.* B **23** 098101
[40] Kostov K L, Gsell M, Jakob P, Moritz T, Widdra W and Menzel D 1997 *Surf. Sci.* **394** L138–44
[41] Malard L M, Pimenta M A, Dresselhaus G and Dresselhaus M S 2009 *Phys. Rep.* **473** 51–87
[42] Ferrari A C *et al* 2006 *Phys. Rev. Lett.* **97** 187401
[43] Sutter P, Sadowski J T and Sutter E A 2010 *J. Am. Chem. Soc.* **132** 8175–9
[44] Ma R S, Huan Q, Wu L M, Yan J H, Zou Q, Wang A W, Bobisch C A, Bao L H and Gao H J 2017 *Rev. Sci. Instrum.* **88** 063704
[45] Fang W *et al* 2013 *Nano Lett.* **13** 1541–8
[46] Qian Y and Kang D J 2018 *ACS Appl. Mater. Interfaces* **10** 29069–75
[47] Liu W, Li H, Xu C, Khatami Y and Banerjee K 2011 *Carbon* **49** 4122–30